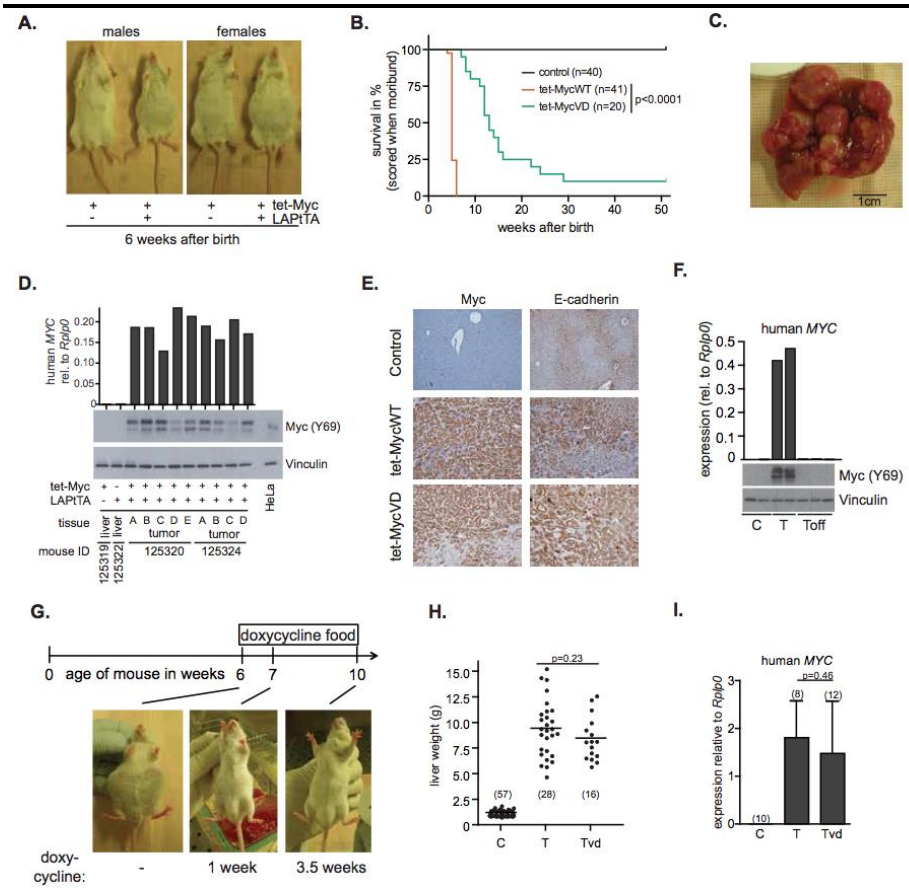


tet-Myc WP1: Figure 1.1

**tet-MycVD is impaired in liver tumor induction compared to tet-MycWT.**

**A.** Representative photos of double-transgenic tet-Myc/LAPtTA mice upon tet-Myc induction in utero, or single-transgenic tet-Myc control mice, showing the increased abdominal size in male and female double-transgenic mice by the age of 6 weeks. **B.** Kaplan-Meier survival curve of tet-MycWT (orange) or tet-MycVD (green) overexpressing, or control (wildtype or single-transgenic, black) mice. Mice were euthanized and scored when moribund. The median survival was 5 weeks for tet-MycWT and 13 weeks for tet-MycVD expressing mice. Significance was assessed using the log-rank test. **C.** Representative photo of a tet-MycWT overexpressing liver containing multiple tumor nodules. **D.** mRNA and western blot analyses of human MYC mRNA (= transgene) and mouse/human Myc protein expression in control liver and tet-MycWT tumor samples. For western blot analyses, the Myc antibody Y69 was used. It recognizes Myc of mouse and human origin. **E.** Representative immunohistochemical stainings of control, tet-MycWT and tet-MycVD samples, using antibodies targeting Myc or E-cadherin. **F.** Human MYC mRNA levels in control (C) livers or tet-MycWT tumors before (T) or after (16h; Toff) doxycycline treatment were assessed by qRT-PCR. For western blot analyses, the Myc antibody Y69 was used (see C.). **G.** Photos of one tet-MycWT expressing mouse at the age of 6 weeks before switching off tet-Myc transgene expression, displaying strong abdominal swellings (left). Providing doxycycline food led to rapid regression of the tumors, as observable on the photos taken after 1 (middle) and 3.5 weeks (right) of treatment. **H.** Liver weight (in grams, g) of control (C), tet-MycWT (T) or tet-MycVD (Tvd) overexpressing mice on the day of euthanasia. Significance was assessed with the student's t- test and p-values are displayed in the figure or as follows: T vs C: 4.6x10-37, Tvd vs C: 2.3x10-37. **I.** qRT-PCR analyses of human MYC mRNA levels in tumors (T or Tvd) or control livers. The numbers in brackets originate from independent replicates. Significance was assessed using the student's t-test.

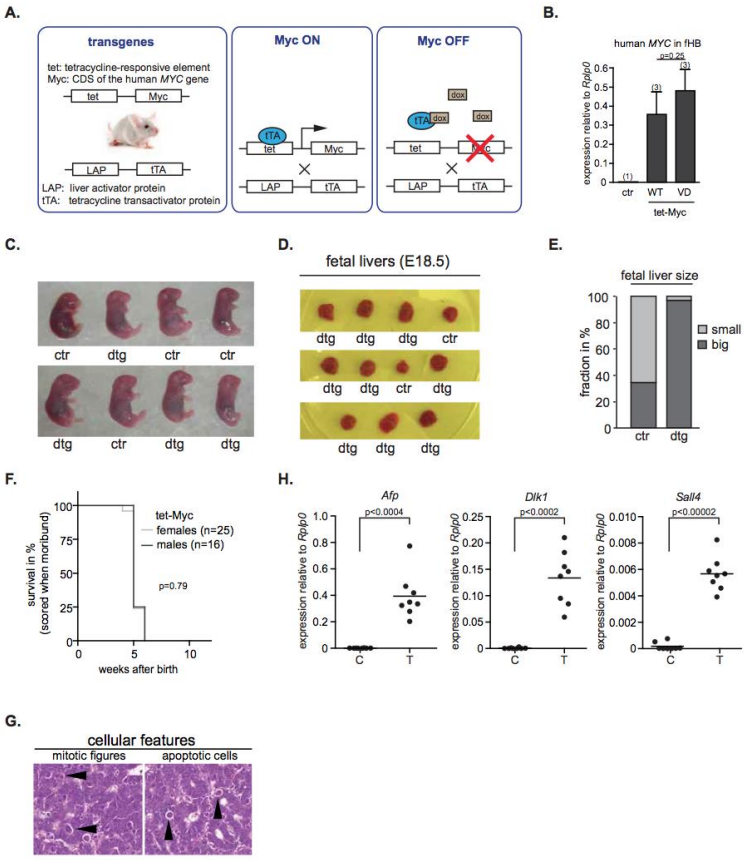


tet-Myc WP1: Supplementary Figure 1.2

**tet-Myc induction in utero leads to fast and highly penetrant tumorigenesis.**
**A.** Schematic overview of the mouse model. Single- transgenic tet-Myc or LAPtTA mice were crossed to achieve tet-Myc/LAPtTA double-transgenic, tet-Myc overexpressing mice (wild-type and single-transgenic mice were used as controls). In the absence of doxycycline (middle), transgene expression was active whereas providing doxycycline-containing food switches off tet-Myc transgene expression (right). CDS: coding sequence. **B.** Fetal hepatoblasts (fHB) from embryonic day E18.5 were purified using anti-E-cadherin antibodies. Human MYC mRNA levels were assessed by qRT- PCR, using Rplp0 as housekeeper. The numbers in brackets result from independent purifications (pool of all embryos of one pregnant female) per genotype. **C.** tet-Myc overexpressing (dtg; double-transgenic for tet-Myc/LAPtTA) or control (ctr; single-transgenic for tet-Myc) embryos at day E18.5. **D.** Representative photos of tet-Myc overexpressing (dtg) or control (ctr; single-transgenic for tet-Myc) embryonic livers at day E18.5. **E.** Embryonic ctr or dtg livers at E18.5 (D.) were assessed for their size and categorized as small or big relative to the average size of each litter (n = 6 litters). **F.** Kaplan-Meier survival curve of tet-Myc expressing female (grey) or male (black) mice (total n=41). Mice were euthanized and scored when moribund. Significance was assessed with the log-rank test. The tet-Myc mouse strain used in this study contains the transgene on an autosome and therefore allows studying mice of both genders (contrary to the originally published mouse strain with the transgene on the Y chromosome. **G.** Representative histological sections (H&E staining) showing examples of mitotic figures (left) and apoptotic cells (right), as indicated by the arrowheads. **H.** mRNA expression values of hepatoblasts markers Afp, Dlk and Sall4, as measured by quantitative RT-PCR. Graphs show average and standard deviation for biological replicates of C (n=8) and T (n=8) samples. Significance was assessed using the student's t-test.

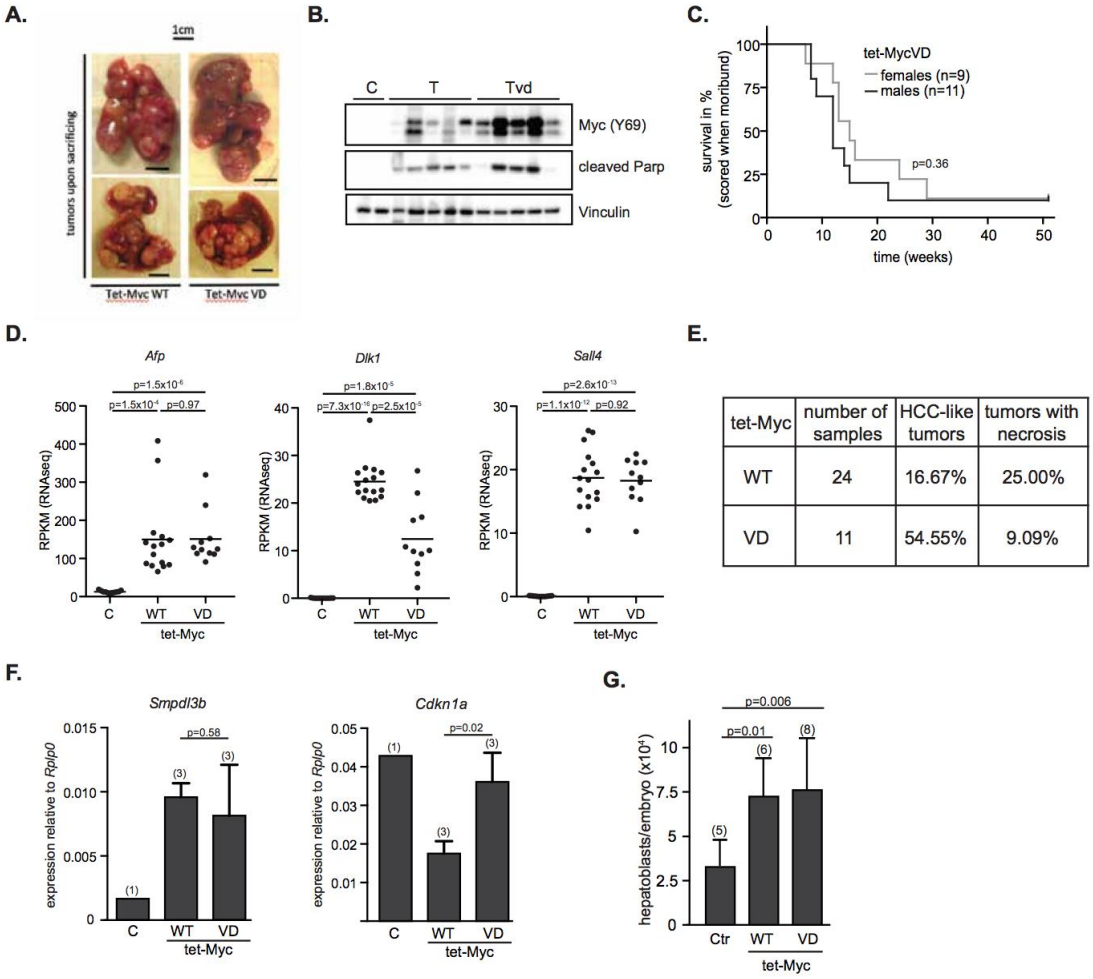


| tet-Myc | number of samples | HCC-like tumors | tumors with necrosis |
|---|---|---|---|
| WT | 24 | 16.67% | 25.00% |
| VD | 11 | 54.55% | 9.09% |

tet-Myc WP1: Supplementary Figure 1.3

**tet-MycWT and tet-MycVD overexpression induces liver tumorigenesis.**

**A.** Photos of tet-MycWT or tet-MycVD overexpressing livers. The scale bars represent 1 cm of length. **B.** Western blot analyses of Myc and cleaved Parp (Asp214) in tet-Myc and tet-MycVD tumors. Vinculin was used as loading control. **C.** Kaplan-Meier survival curve of tet- MycVD overexpressing male (black) or female (grey) mice. Mice were euthanized and scored when moribund. Median survival was 12 weeks for males and 15 weeks for females, but the difference between the genders in tumor survival was not significant, as assessed by log-rank test. **D.** mRNA expression (as measured by RNA-seq) of fetal hepatoblasts markers Afp (left), Dlk1 (middle) and Sall4 (right) in control liver (C) and tet-MycWT (T) or tet-MycVD (Tvd) tumors. Significance was assessed with the student's t-test. **E.** Tet-Myc induced liver tumors are histologically classified as hepatoblastoma or HCC-like tumors. This table gives the percentages of HCC-like tumors among the tet-MycWT or tet-MycVD induced nodules as well as the fraction of tumors containing necrotic areas. **F.** mRNA expression of Smpdl3b and Cdkn1a in control (C), tet-MycWT (WT) or tet-MycVD (VD) overexpressing fetal hepatoblasts (fHB) at embryonic day E18.5. Significance was assessed with the student's t-test. **G.** Numbers of E-cadherin positive purified fHB are plotted as cells per embryo. The numbers in brackets display the number of pregnant females from which the fHB were purified. Significance was assessed with the student's t-test.

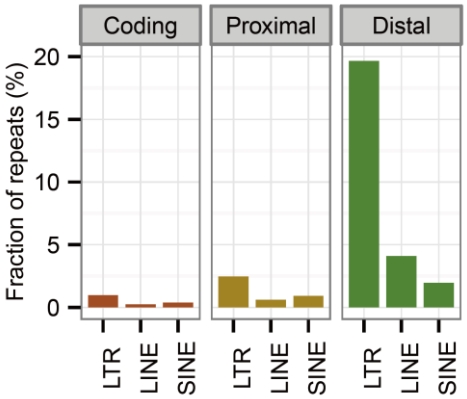


**Figure 2.1.** Fraction of repetitive elements.

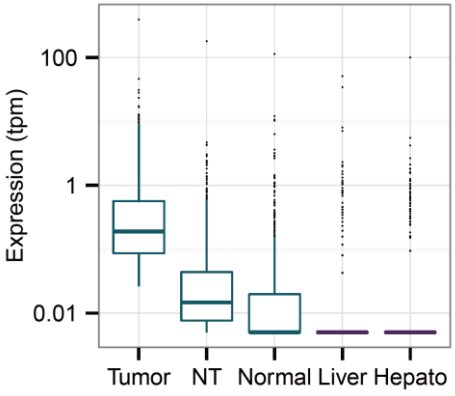


**Figure 2.2.** Expression levels of LTRs

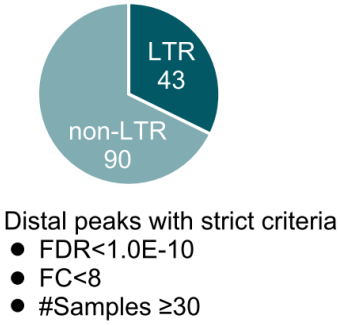


**Figure 2.3.** Fraction of LTR-derived top ncRNAs

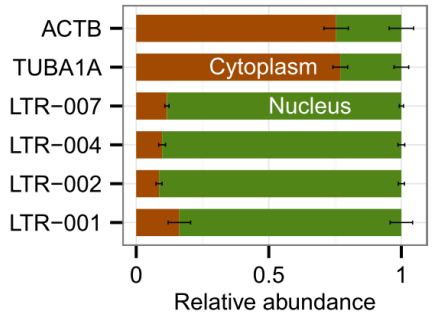


**Figure 2.4.** Relative abundance of four LTR ncRNAs

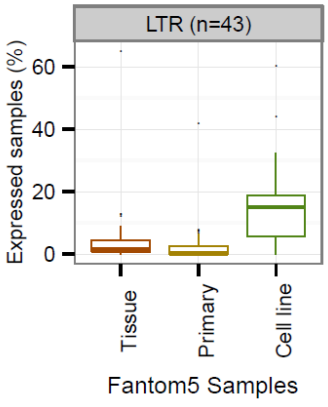


**Figure 2.5.** Proportion of samples that express the LTRs

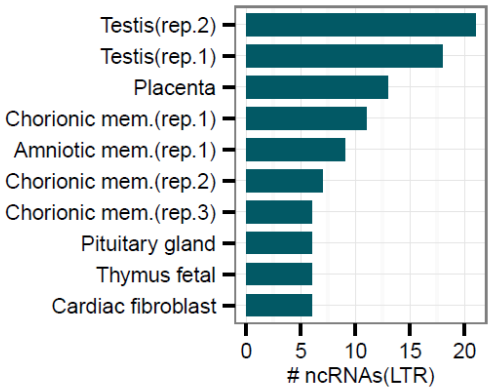


**Figure 6.** Top10 tissues that express the top LTRs

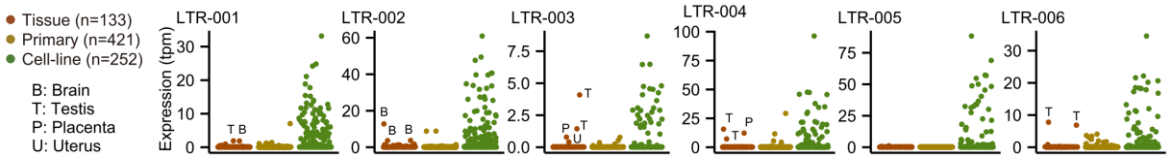


**Figure 2.7.** Expression patterns of the top 6 LTRs in human primary cells, tissues, and cancer cell-lines.

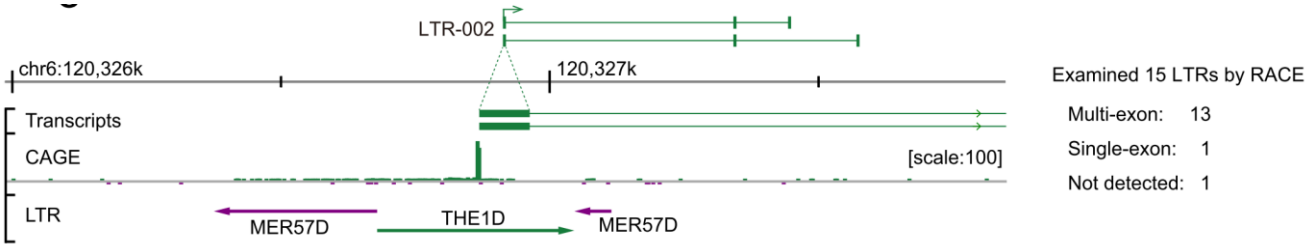


**Figure 2.8.** Full-length ncRNAs with LTR promoters determined by 3' RACE.

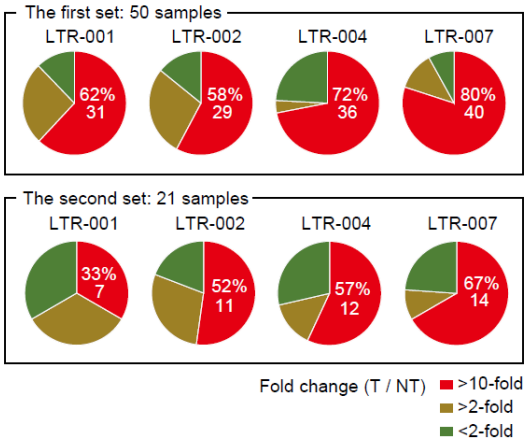


**Figure 2.9.** Fold changes of four LTRs by qPCR

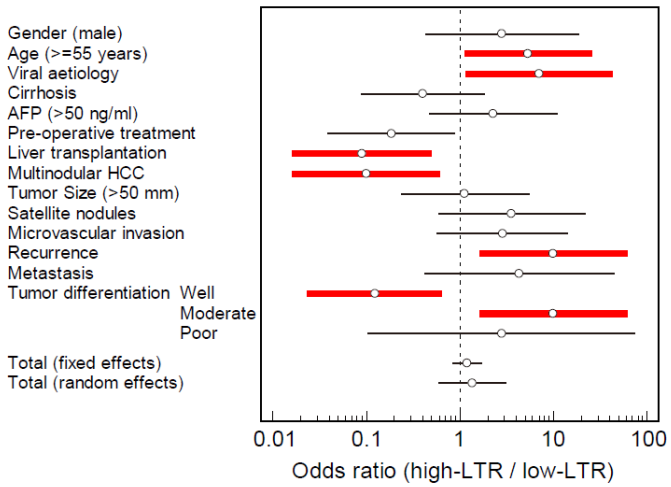


**Figure 2.10.** Clinical features associated with LTR expressions

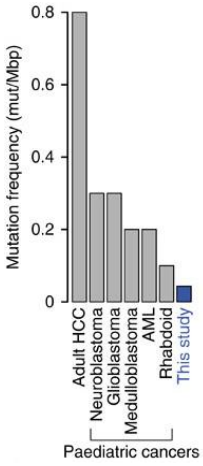


**Figure 2.11.** Non-silent mutations frequency in BSEP-HCCs (This study) compared with adult HCCs and other paediatric non-hepatic cancers.

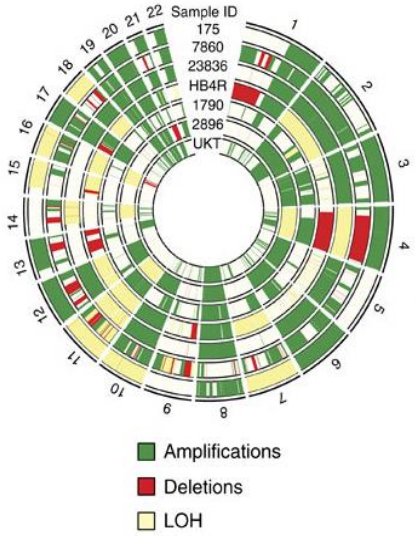


**Figure 2.12.** Circos plot reporting amplifications, deletions and loss of heterozygoty (LOH) in all chromosomes of the seven BSEP-HCCs.